Last changed: October 1, 2018

Propynal, an Interstellar Molecule with an Exceptionally Strong C≡C Infrared Band - Laboratory Infrared Data and Applications

by

Reggie L. Hudson and Perry A. Gerakines

Astrochemistry Laboratory (Code 691),
NASA Goddard Space Flight Center, Greenbelt, MD 20771 USA

ABSTRACT

Isomers with the formula C_3H_2O have intrigued and puzzled astronomers and astrochemists for many years, with propynal and cyclopropenone, but not propadienone, known to be interstellar. However, there is a severe lack of laboratory spectra of the solid phases of these compounds with which to investigate their interstellar chemistry. Here we present the first infrared spectra of amorphous and crystalline forms of propynal, HCC-C(O)H, at multiple temperatures. Band positions are tabulated and band strengths are derived in terms of absorption coefficients and integrated intensities. Optical constants are calculated for amorphous propynal, refractive indices are measured, and densities are estimated. Three laboratory astrochemistry applications are described, including a new spectral identification in an earlier paper. It is shown that propynal's C≡C infrared absorbance is about 30,000% stronger than the corresponding feature in acetylene. This band's intensity and spectral position make it an attractive candidate for astronomical searches involving interstellar ices.

Key words: ISM: molecules – methods: laboratory: molecular – methods: laboratory: solid state – astrochemistry.

E-mail: reggie.hudson@nasa.gov

1 INTRODUCTION

The three C_3H_2O isomers in Fig. 1 continue to interest laboratory, observational, and theoretical astrochemists (Loomis et al. 2015). Studies have shown that propynal and propadienone have about the same energy with cyclopropenone much higher, but only propynal and cyclopropenone have been found in the interstellar medium (Irvine et al. 1988; Hollis et al. 2006; Loison et al. 2016). Gas-phase spectral measurements have been made on all three compounds, and models proposed to explain their formation (e.g., Quan & Herbst, 2007). However, it is difficult to explain the observed interstellar abundances of these C_3H_2O molecules with only gas-phase reactions, and so solid-phase syntheses in interstellar ices have been proposed for the formation of these isomers (Zhou et al. 2008). See McCarthy et al. (2017) for a good summary of these issues.

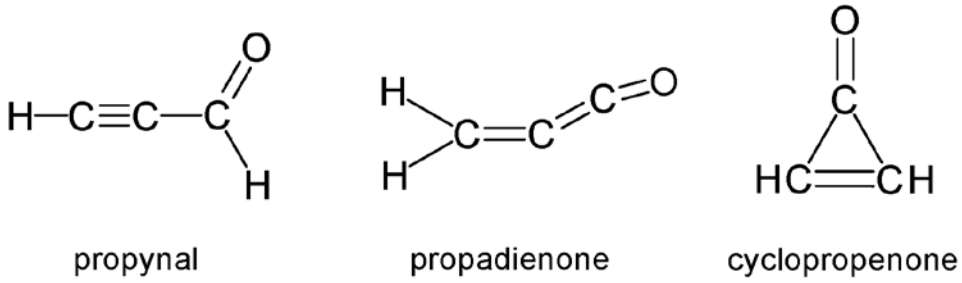

Figure 1. Three C_3H_2O isomers. See Costain & Morton (1959), Brown et al. (1985), Benson et al. (1973), and references therein for structural details.

Several paths to interstellar propynal, the molecule of interest in the present paper, have been suggested. In their discovery paper for propynal in the Taurus Molecular Cloud 1 (TMC-1), Irvine et al. (1988) favored a path involving gas-phase formation from the ion-molecule reaction of CO and protonated acetylene. This reaction was subsequently questioned by Petrie (1995), who suggested a radical-neutral combination involving C_2H and H_2CO as an alternative. A photolytic path of $C_3 + H_2O \rightarrow$ propynal was described by Ekern et al. (1996) for ice mantles of interstellar dust grains, while Xie et al. (2007) later argued for a reaction of C_3H on amorphous H_2O-ice to make propynal, with the ice catalyzing the reaction by lowering its activation barrier. Zhou et al. (2008) reported results of laboratory experiments on electron-irradiated CO + C_2H_2 ices, and assigned to propynal two weak infrared (IR) peaks seen to grow into the ice's spectrum. The case for a combination of gas-phase and grain-surface processes involving $O + C_3H_3 \rightarrow$ propynal was made in this journal by Loison et al. (2016), who presented a detailed summary of proposed C_3H_2O syntheses. In short, multiple lines of theory and experiment have been used to address the formation of interstellar propynal. Aside from the initial discovery in TMC-1, we note that this

molecule also has been reported in objects such as Sagittarius B2, star-forming regions, and starless cores (e.g., Turner 1991; Loomis et al. 2015; Loison et al. 2016).

In the present paper we focus on the first of the C_3H_2O isomers in Fig. 1, propynal, which we write as HCC-C(O)H to emphasize the two distinct functionalities of the molecule, the HCC- (alkynyl) and -C(O)H (formyl) groups. Despite the fact that propynal was first isolated over a century ago (Claisen 1898) and that commercial infrared spectrometers have been available since the 1940s (Wilks 1986), we are unable to find a single conventional mid-IR transmission spectrum of propynal in the literature. While we cannot say with certainty that no such published spectra exist, our inability to locate them argues for their scarcity. The earliest propynal IR paper we have found is that of Brand & Watson (1960) who tabulated band positions and assigned various spectral features, but did not show the IR spectrum of HCC-C(O)H. A more-detailed study followed, but again no IR spectrum was presented (Brand et al. 1963). A paper by King & Moule (1961) included one HCC-C(O)H spectrum, but without either a label or numbers on the intensity axis (vertical axis), just what was plotted is unknown. See also the gas- and solution-phase work of Klaboe & Kramer (1971). To date, the only IR spectrum of solid propynal we have found is in the recent paper of Jonusas et al. (2017), but the molecule's three strongest IR features are off the scale of the figure presented. Only one spectrum was shown, for a single ice thickness and only one temperature, and it was recorded in a reflection mode, not transmission, making intensity comparisons difficult (Pacansky & England 1986).

This lack of IR data on propynal hinders explorations into the astrochemistry of this molecule and its C_3H_2O isomers. One example of this problem is the work of Zhou et al. (2008), already mentioned. Those authors examined propynal formation in a C_2H_2 + CO ice, but they were forced to rely, in part, on gas-phase IR data to make spectral assignments for their solids, a less than desirable approach, but one that was perhaps difficult to avoid at the time. In the work of Jonusas et al. (2017), also already mentioned, an indirect method had to be used to estimate the ice's abundance (i.e., column density of propynal molecules) due to a lack of published IR band strengths for the molecule. In our own laboratory, we have been hampered by a lack of published information on propynal and other aldehydes while studying the low-temperature chemistry and spectroscopy of simple alcohols.

To address the paucity of IR data for this interstellar molecule, here we report new results on solid HCC-C(O)H at 10 - 150 K. Infrared spectra of amorphous and crystalline propynal are presented at multiple temperatures, along with measurements of refractive indices at 670 nm and calculations of densities. Band strengths and absorption coefficients are given for seven IR features of propynal. Infrared optical constants, *n* and *k*, are calculated from which both apparent and absolute band strengths can be derived. Temperatures are given for crystallization and sublimation, and several astrochemical applications are described.

2 EXPERIMENTAL SECTION

Propynal was purchased from Santa Cruz Biotechnology and used as received, other than degassing with liquid nitrogen and three freeze-pump-thaw cycles. Undesired loss of propynal resulted from either repeated freeze-pump-thaw cycles or sparging with helium, so that it was difficult to remove all dissolved atmospheric gases. The purchased sample's brown-red color, due to slow polymerization, could be removed by vacuum-line distillation, but we found that this was not necessary due to our sample preparation method (see below) and made no difference in the results reported here.

Safety Note! Propynal is both a mutagen and a lachrymatory agent. Warnings about its possible polymerization and explosive nature are in the literature (e.g., Seburg et al. 2009). Caution is urged in its use.

Ices were prepared by vapor-phase depositions onto a precooled KBr window at a rate that gave an increase in the ice's thickness of 1 - 2 μm hr^{-1}, with thicknesses being determined by laser interferometry (Groner et al. 1973). Mid-infrared spectra (6000 - 400 cm^{-1}) of the resulting samples were recorded in transmission with a Thermo iS50 infrared spectrometer interfaced to a closed-cycle ARS cryostat (T_{min} ~ 9 K) and a vacuum system (P_{min} ~ 10^{-8} torr at room temperature). Spectra recorded at multiple resolutions showed few differences for 0.5, 1.0, and 2.0 cm^{-1} settings, so the latter was used in most cases. The IR beam of the spectrometer was unpolarized and perpendicular to the KBr window. See our earlier papers for more details (e.g., Gerakines & Hudson 2015a, 2015b).

Reference spectra of solid propyne (Sigma Aldrich) were recorded with the Thermo spectrometer and associated equipment already mentioned. A few experiments were done in which amorphous HCC-CH_2OH, propargyl alcohol (Sigma Aldrich), was irradiated at 20 K with 1 MeV protons. Again, see our earlier papers for details of the proton source, dose calculations, the in situ IR measurements, and so forth (e.g., Hudson and Loeffler 2013; Hudson 2016).

Density-functional theory (DFT) calculations at the B3LYP/6-31+G* level, carried out with Spartan software (Wavefunction, Inc., Irvine, California, USA), assisted in assigning ^{13}C peaks and visualizing propynal vibrations.

3 RESULTS

3.1 Refractive indices and densities

Interference fringes recorded during deposition were used to determine each sample's thickness (*h*) through

$$h = \frac{N_{fr}\lambda}{2\sqrt{n^2 - \sin^2\theta}} \quad (1)$$

where N_{fr} was the number of fringes recorded, λ = 670 nm, n was the ice's refractive index at 670 nm, and $\theta \approx 0°$, the angle made by the laser's light with respect to a line drawn perpendicular to the ice's surface (Heavens 2011). In turn, the refractive indices of propynal needed in equation (1) were measured by two-laser interferometry (Tempelmeyer & Mills 1968; Moore et al. 2010; Luna et al. 2012). Triplicate measurements gave n_{670}(10 K) = 1.37 ± 0.01 and n_{670}(125 K) = 1.52 ± 0.01 for amorphous and crystalline propynal, respectively. Using bond polarizabilities (Denbigh 1940), propynal's specific refraction (r) was calculated to be 0.2394 $cm^3\ g^{-1}$, within ~5% of the value found from the room-temperature data of Veliev and Guseinov (1980). Substituting r and our n_{670} results into the Lorentz-Lorenz relation

$$\rho = \left(\frac{1}{r}\right)\left(\frac{n^2 - 1}{n^2 + 2}\right) \qquad (2)$$

gave densities of ρ = 0.945 and 1.270 g cm^{-3} for amorphous and crystalline propynal, respectively. These n_{670} and ρ values were used to determine ice thicknesses and IR band strengths and absorption coefficients.

We estimate that the uncertainties in our measured n_{670} values are near 1%, as in our acetylene work (Hudson et al. 2014a), but that our calculated density (ρ) values for propynal are uncertain to ~5% due to the uncertainty in the specific refraction (r) already mentioned. These estimates carry over into an uncertainty near 1% for our absorption coefficients (α) values, but ~5% for the band strengths (A'). A more direct density measurement could lower this 5% considerably.

3.2 Infrared spectra

The propynal molecule has the planar structure shown in Fig. 1, but with the CCC bond bent at the middle carbon by ~1.6° from linearity and away from the oxygen atom (Costain & Morton 1959; Barros et al. 2015). Since propynal has N = 6 atoms, there are 3N - 6 = 3(6) - 6 = 12 fundamental vibrations and, under the C_s point group, these correspond to nine a' (totally symmetric) types and three a" types, all being IR active. Ten of these twelve fundamentals were within the range of our equipment and were detected.

Fig. 2 shows survey spectra of amorphous propynal at 10 K, the temperature at which the ice was prepared, and after warming to 100 K (thickness ≈ 1 μm). Only slight spectral differences, all irreversible, were seen with this temperature increase, but continued warming to 115 K produced distinct splittings and shifts of IR peaks, common signs of crystallization. The only significant change in peak positions above 115 K was a slow irreversible shift of the carbonyl (C=O) peak at 1665 cm^{-1} to about 1650 cm^{-1} at 135 K, which continued to about 1644 cm^{-1} at 145 K, at which temperature the ice was

subliming from the substrate. No residue remained on the KBr substrate after this warming sequence.

Our main interest in this paper is amorphous propynal-containing ices as it seems unlikely that propynal in astronomical environments could be sufficiently abundant to form crystals. Nevertheless, the IR literature on solid propynal is so scarce that we believe it important to report a few measurements on the crystalline compound. Therefore, in Fig. 3 we use expanded scales to compare the spectrum of crystalline propynal, made by a deposition at 125 K, with the spectrum of the 10 K amorphous ice of Fig. 2. Cooling the 125 K sample gave a few shifts in line positions and shapes, but little else. The main difference in the propynal spectra obtained by (i) deposition at 10 K and subsequent warming to 125 K and (ii) deposition at 125 K was in the carbonyl band around 1650 cm^{-1}. Its position in Fig. 3 was about 1645 cm^{-1}.

Table 1 lists the positions of selected fundamental bands of 10 K amorphous and 125 K crystalline propynal, from Fig. 3. Assignments and descriptions, based on the gas-phase work cited in the table's footnote, are given with the understanding that these are simplifications of the actual molecular motions. We are not aware of any such tables or spectra for solid propynal in the literature. Aside from our tabulated peak positions for amorphous propynal, we also found ^{13}C satellites for the ν_3(C≡C stretch), 2077 cm^{-1} for H^{13}C≡^{12}C- and 2053 cm^{-1} for H^{12}C≡^{13}C-, and for the ν_4(C=O stretch), 1630 cm^{-1} for ^{13}C=O, best seen in the middle panel of Fig. 3. A peak at 3051 cm^{-1} was assigned to the $\nu_4 + \nu_5$ combination band, while weak peaks at 2749 and 1984 cm^{-1} were assigned to the $2\nu_5$ and $2\nu_6$ overtones, respectively. No attempt was made to assign all such weak IR features.

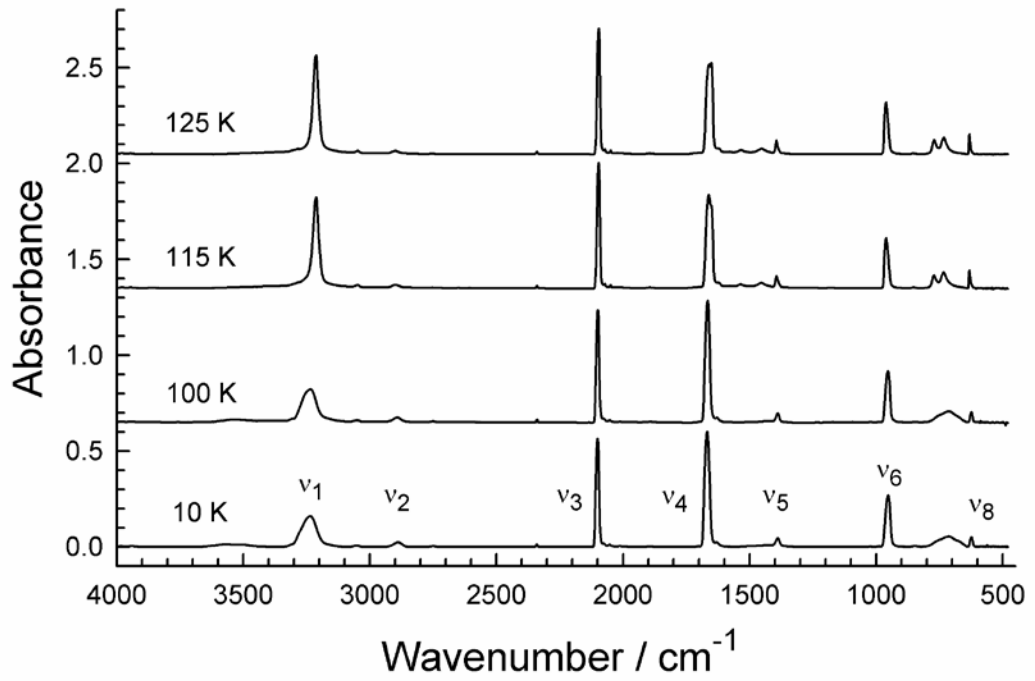

Figure 2. Infrared survey spectra of propynal deposited at 10 K and then warmed to 100, 115, and 125 K. The thickness of the 10 K ice was about 1 μm. Spectra have been offset vertically for clarity. Seven fundamental vibrational bands of propynal are as indicated.

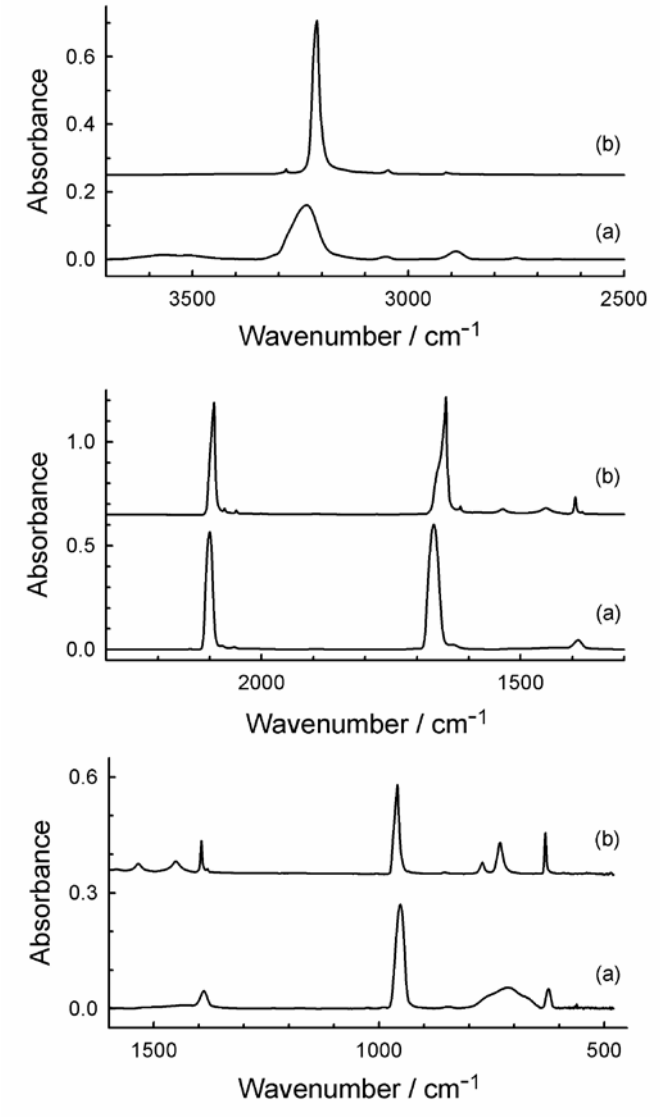

Figure 3. Comparison of IR spectra of (a) amorphous and (b) crystalline propynal. The amorphous ice was made, and its spectrum recorded, at 10 K. The crystalline ice was made, and its spectrum recorded, at 125 K. Thicknesses were about (a) 1.0 and (b) 0.32 μm. Spectra have been offset vertically for clarity.

Table 1

Positions (cm^{-1}) of Some Propynal Vibrations

Vibrational mode and symmetry type	Approximate motion [a,b]	Amorphous, 10 K, IR [c]	Crystalline, 125 K, IR [c]	Gas, IR [d]
ν_1 a'	H-C≡ stretch	3234	3212	3326
ν_2 a'	=C-H stretch	2889	2914	2858
ν_3 a'	C≡C stretch	2099	2092	2106
ν_4 a'	C=O stretch	1666	1644	1697
ν_5 a'	=C-H wag (ip)	1387	1394	1389
ν_6 a'	C-C stretch	952	959	944
ν_7 a'	H-C≡ wag (ip)	713	732	650
ν_8 a'	H-C≡C bend (ip)	624	631	614
ν_9 a'	C≡C-C bend (ip)	---	---	205
ν_{10} a''	C(O)H wag (op)	989	1006	981
ν_{11} a''	H-C≡ wag (op)	756	771	693
ν_{12} a''	C≡C-C bend (op)	---	---	261

[a] Assignments and descriptions are from the gas-phase work **of** Lin and Moule (1971), Brand et al. (1963), and references therein. Some variations exist for assignments, descriptions, and positions of ν_7, ν_8, and ν_{11}. See also King and Moule (1961) and McKellar et al. (2008).

[b] ip = in plane, op = out of plane

[c] This work.

[d] Brand et al. (1963).

3.3 Infrared band intensities and optical constants

Propynal ices with thicknesses ranging from about 0.1 to 1.5 μm were prepared, and band areas and peak heights measured for the seven IR features labeled in Fig. 2. Appropriate Beer's law plots were constructed and their slopes used to extract apparent absorption coefficients (α') and apparent band strengths (A') covering most of the wavenumber range shown in Figs. 2 and 3 (Hollenberg & Dows 1961; Gerakines & Hudson 2015b). Tables 2 and 3 summarize the results. We note that all Beer's law graphs had correlation coefficients of at least 0.995 and that neither peak positions, band shapes, nor relative intensities varied with thickness.

Table 2

Intensities for Selected IR Features of Amorphous Propynal at 10 K [a]

Vibration [b]	Position / cm^{-1}	α' / cm^{-1}	Integration Range / cm^{-1}	A' / 10^{-18} cm $molecule^{-1}$
ν_1	3234	3630	3350-3100	26.6
ν_2	2889	582	2945-2820	2.06
ν_3	2099	12700	2120-2080	18.2
ν_4	1666	13300	1700-1640	28.0
ν_5	1387	1020	1414-1360	1.59
ν_6	952	5970	980-900	13.0
ν_8	624	1170	640-605	1.31

[a] n_{670} = 1.37, ρ = 0.945 g cm^{-3}; α' and A' rounded to 3 significant figures in most cases

[b] Assignments are from the gas-phase work **of** Lin and Moule (1971), Brand et al. (1963), and references therein. See also King and Moule (1961) and McKellar et al. (2008).

Table 3

Intensities for Selected IR Features of Crystalline Propynal at 125 K [a]

Vibration [b]	Position / cm^{-1}	α' / cm^{-1}	Integration Range / cm^{-1}	A' / 10^{-18} cm $molecule^{-1}$
ν_1	3212	4040	3270-3150	53.8
ν_2	2914	468	2930-2890	0.32
ν_3	2092	37900	2120-2075	30.2
ν_4	1644	37900	1700-1625	43.1
ν_5	1394	6640	1410-1384	1.91
ν_6	959	14800	980-940	14.4
ν_8	631	8050	640-605	3.37

[a] n_{670} = 1.52, ρ = 1.270 g cm^{-3}; α' and A' rounded to 3 significant figures in most cases

[b] Assignments are from the gas-phase work **of** Lin and Moule (1971), Brand et al. (1963), and references therein. See also King and Moule (1961) and McKellar et al. (2008).

Optical constants (*n* and *k*) were determined for amorphous propynal as in our recent papers on CH_4 and CO_2 (Gerakines & Hudson 2015a; Gerakines & Hudson 2015b), and are shown in Fig. 4. With optical constants one can calculate IR spectra for a range of ice thicknesses and experimental configurations, such as transmission through a substrate or reflection from a mirror. Such constants find widespread use in the planetary science community, whereas band strengths are more commonly used by interstellar astrochemists. The equation $\alpha = 4\,\pi\,k\,\tilde{\nu}$ gives absolute absorption coefficients (α), and integrations of these α values give absolute band intensities (*A*). – For the difference in apparent and absolute band strengths, and apparent and absolute absorption coefficients, see Hudson et al. (2014a, 2014b) or Molpeceres et al. (2017) and reference therein. – Values of *n* and *k* for amorphous propynal are posted on our web pages at https://science.gsfc.nasa.gov/691/cosmicice/constants.html.

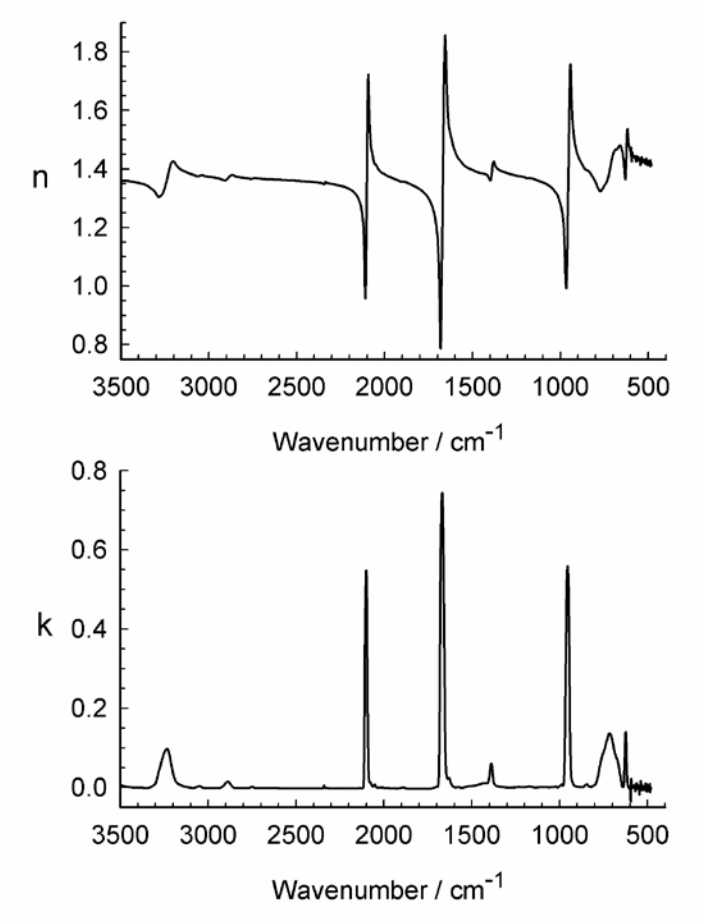

Figure 4. Optical constants *n* and *k* for amorphous propynal at 10 K.

Our optical constants calculations required ice thicknesses to be known, which were found with our n_{670} values of propynal. However the main contributor to uncertainty in *n* and *k* was the uncertainty in the refractive index of the substrate, KBr, which was thought to be no more than about 5%. Our values of *k* can be relied on down to a lower limit of about $k = 1 \times 10^{-4}$, below which the influence of the background noise becomes significant.

3.4 Other results

For comparison purposes we also recorded IR transmission spectra of propyne and propynal, HC≡C-CH_3 and HC≡C-C(O)H, respectively, at the same temperature and with the same equipment. The results for two regions of interest are shown in Fig. 5, each spectrum scaled vertically (normalized) to fit half of the figure. Note the substantial change in relative intensity of the C≡C peak, compared to the H-C≡ peak, on going from the upper spectrum compared to the lower one. We return to this point in our Discussion.

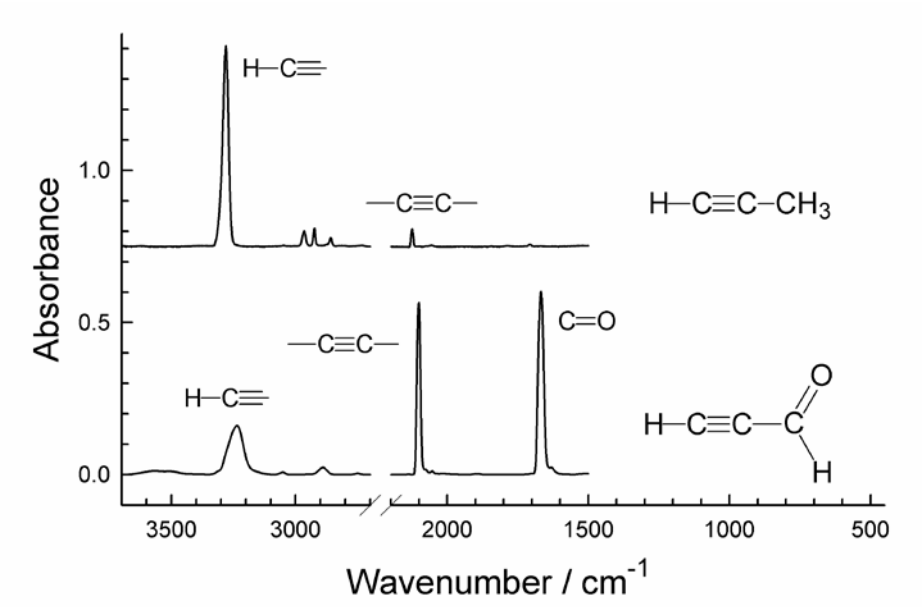

Figure 5. Infrared spectra of amorphous propyne (top) and amorphous propynal (bottom) each ice made, and its spectrum recorded, at 10 K. The thickness of each sample was ~1 μm. Spectra have been offset for clarity.

Several ices were prepared in which propynal was mixed with H_2O-ice, co-depositing the two compounds at 10 K through separate calibrated deposition lines, the flow rates being adjusted to give a final number ratio of (H_2O:propynal) ~ 20:1. Perhaps the most significant thing about the resulting IR spectrum was that propynal's C≡C stretch remained strong and clearly visible at 2101 cm^{-1}, close to the 2099 cm^{-1} value in

neat propynal. Other positions in amorphous H_2O-ice (neat propynal in parentheses) were 1663 (1666), 1391 (1387), and 960 (952) cm^{-1}. These four propynal peaks could be seen on warming this mixed ice above the amorphous H_2O's crystallization (~140 K) and even up to the H_2O-ice's sublimation (~170 K).

In a final experiment, we irradiated amorphous propargyl alcohol ($HC{\equiv}C\text{-}CH_2OH$) at 20 K with ~1 MeV protons to simulate the influence of low-energy cosmic rays on this compound, which Pearson & Drouin (2005) described as an "excellent candidate" to be interstellar. Fig. 6 shows propargyl alcohol's IR spectrum from 2300 to 1550 cm^{-1} before and after the irradiation. Comparing traces (a) and (b) one finds that the IR peak near 2121 cm^{-1}, for the alcohol's C≡C stretch, decreases in size on irradiation and that this change is accompanied by the growth of two large peaks in (b). These two new peaks, near 2100 and 1666 cm^{-1}, are matched by the two large peaks in the propynal reference spectrum at the bottom of the figure. Additional details and assignments**,** as well as other reaction products**,** will be given in a separate paper, the point here being simply that propynal forms on irradiation of propargyl alcohol. – See Nyquist (1971) for propargyl alcohol IR assignments, but note that the $\nu_{C{\equiv}O}$ in his Table 1 should be $\nu_{C{\equiv}C}$ as propargyl alcohol does not have a C≡O bond.

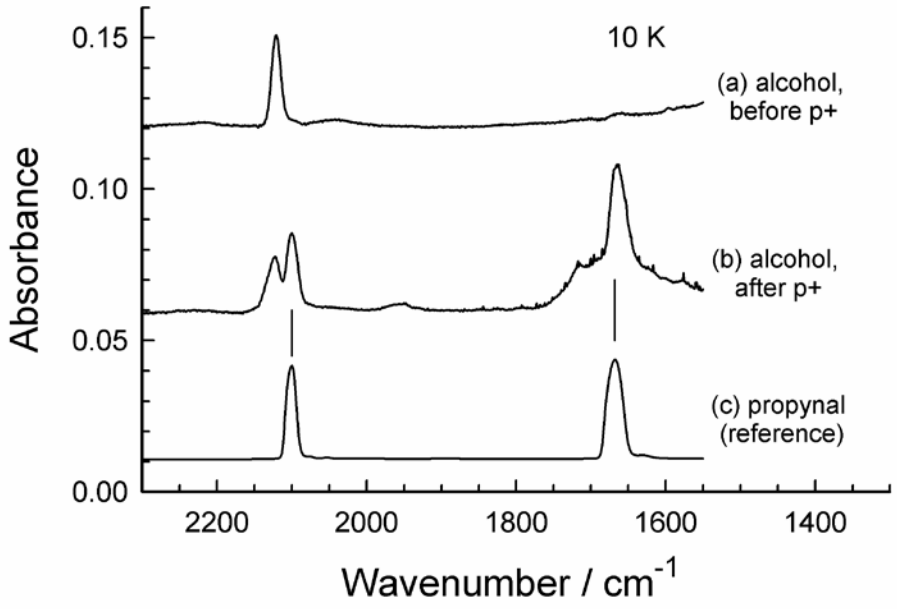

Figure 6. Infrared spectra of amorphous propargyl alcohol at 10 K (a) before and (b) after irradiation to a dose of ~3.5 eV $molecule^{-1}$ with 1 MeV H^+, compared to (c) a reference spectrum of amorphous propynal at 10 K, scaled vertically to roughly match the middle spectrum. Spectra have been offset for clarity. Small spikes in the middle spectrum between about 1800 and 1550 cm^{-1} are due to the incomplete removal of atmospheric H_2O outside the sample chamber.

4 DISCUSSION

4.1 Refractive indices and densities

Little comparison data are available for solid propynal's densities and refractive indices. However, since amorphous solids are sometimes considered to be frozen liquids, our density of ρ = 0.945 g cm^{-3} seems reasonable when compared to the liquid-phase value of ρ = 0.9160 g cm^{-3} (Veliev & Guseinov 1980). Moreover, our *n*(16 K) = 1.37 for the amorphous solid also seems reasonable given that *n* = 1.4065 for liquid propynal at 20 °C (Veliev & Guseinov 1980). For the crystalline compound, we found *n* = 1.52 for a crystalline-amorphous difference of Δn = 1.52 - 1.37 = 0.15, which is similar to that for several other compounds we have studied, such as C_2H_2, C_2H_6, N_2O, and acetone (Hudson et al. 2014a, 2014b, 2017, 2018).

4.2 Infrared spectra

Amorphous propynal's IR spectrum in Fig. 2 is close to what one would expect, with five distinct features from the H-C≡C and H-C(O) carbon-hydrogen stretching vibrations followed by C≡C, C=O, and C-C stretches. Evidence for five bending vibrations also was found, and wavenumber positions for all of these fundamentals are listed in Table 1. Of the bending modes, ν_7, ν_{11}, and ν_8 have been challenging in studies of the IR spectrum of propynal vapor (McKellar et al. 2008), and so we suspect that our positions for those three bands may be less firm than for the other fundamentals.

Infrared intensities of seven propynal features are given in Tables 2 and 3, the missing three features being the ν_{10} vibration, which was too weak to reliably integrate, and the ν_7 and ν_{11} vibrations, which were blended. With these seven sets of mid-IR intensities it is possible to derive band strengths of near- and far-IR features of propynal by appropriate scaling. See Richey & Gerakines (2012) and Giuliana et al. (2014) for examples.

The most striking feature of propynal's IR spectrum is the large intensity of the C≡C feature near 2100 cm^{-1}. A quantitative comparison to other molecules can be made by considering the series acetylene, propyne, and propynal (HC≡CH, HC≡C-CH_3, and HC≡C-C(O)H, respectively). For acetylene, our optical constants (Hudson et al. 2014a) can be used to calculate the H-C≡ and C≡C band strengths in Table 4. Also listed are *A*' for the corresponding vibrations of propyne, estimated from the upper spectrum of Fig. 5, and two values for propynal taken from Table 2. It is seen that the IR band strength for the H-C stretch varies but little in these molecules, while *A*' for the C≡C stretch rises by ~3,000% (factor of ~30) on going from propyne to propynal and ~30,000% (factor of ~300) on going from acetylene to propynal.

Table 4

Intensities for Two IR Features in Amorphous Ices at 10 K

Molecule	Formula	*A*' (H-C≡) / 10^{-18} cm molecule^{-1}	*A*' (C≡C) / 10^{-18} cm molecule^{-1}
acetylene [a]	HC≡CH	22.4	0.062
propyne [b]	HC≡C-CH_2-H	22.1	0.621
propynal [c]	HC≡C-C(=O)-H	26.6	18.2

[a] Calculated from optical constants of Hudson et al. (2014a) .

[b] Calculated from the upper spectrum of Fig. 5.

[c] From Table 2.

This intensity enhancement for propynal was not entirely unexpected, with at least two contributing factors at work. First, the IR band strength of a molecular vibration is proportional to the square of the change in the molecule's dipole moment caused by the vibration. Acetylene's ν_2(C≡C) stretching motion involves no dipole moment change, and so is formally IR-forbidden in the gas phase and only weakly present in the amorphous solid. The corresponding C≡C vibration's intensity is greater in propyne as a hydrogen atom in acetylene is replaced by a -CH_3 (methyl) group, resulting in a loss of symmetry. However, the replacement of propyne's -CH_3 group by the highly-polar formyl group, -C(O)-H, on going to propynal results in a greater dipole moment change during the C≡C bond's stretch. In fact, the band strength (*A*') of propynal's C≡C feature is comparable to the most intense features of nearly all molecules in our published work, the strong absorbers CO_2 and N_2O being exceptions (Gerakines and Hudson 2015b; Hudson et al. 2017).

A second factor contributing to the large intensity of propynal's C≡C infrared feature is that the molecule is conjugated, meaning that it has an alternation of single and multiple bonding, in this case a C≡C triple bond and a C=O double bond separated by a C-C single bond. The spectral atlas of Pouchert (1997) can be consulted for liquid-phase examples of this effect, such as the substantial rise in C≡C infrared intensity on going from HC≡C-CH_2-OCH_3 to HC≡C-C(O)-OCH_3 (methyl propargyl ether and methyl propiolate). The latter molecule involves conjugation, but not the former, analogous to the propynal/propyne pair in Fig. 5. See Allan et al. (1955) and Grindley et al. (1974) for a discussion and many liquid-phase examples.

As already stated, our optical constants of amorphous propynal permit the calculation of IR spectra for various ice thicknesses. Integrations of our *k* values, after appropriate conversions, produce absolute band intensities, *A* (Gerakines & Hudson

2015b). It also is possible to use our optical constants to calculate spectra of solid propynal recorded by reflection off of a substrate at various angles, provided the substrate's optical constants also are known.

4.3 Connections to previous and future astrochemical work

Many aspects of our work are relevant to astrochemical research. For example, we have shown that the C≡C stretch of propynal is unusually strong compared to vibrational intensities of many other molecules, and that its position hardly changes when H_2O-ice is either present or absent. We also have shown that propynal is retained in H_2O-ice up to that solid's sublimation. The ^{13}C features we have documented for propynal can be useful in laboratory experiments to make and identify propynal using isotopically labeled reagents. There is even a link to astrobiology as Dowler et al. (1970) have demonstrated that propynal can serve as a precursor to several biomolecules, including nicotinamide and nicotinic acid.

Connections also exist between our new results and several more recent publications.

Zhou et al. (2008) combined infrared spectroscopy, mass spectrometry, computational chemistry, and a kinetic analysis to study the formation of C_3H_2O isomers in an electron-irradiated CO + C_2H_2 (1:1) ice mixture. The spectroscopic evidence for the production of cyclopropenone, propynal, and, tentatively, propadienone in the ice rested on assignments of IR features to those three molecules, but no reference spectra of those molecules were shown. Identifications were based on a combination of peak positions reported for gas-phase, liquid-phase, solid-phase, and matrix-isolated compounds. Our propynal work shows that some of the positions of this molecule's IR features can change substantially with environment, particularly from the gas phase to solid phase, raising questions about the assignment of IR peaks to propynal by Zhou et al. (2008). Reference spectra of propynal in CO + C_2H_2 (1:1) ices could help strengthen the propynal assignment.

In the recent paper of Jonusas et al. (2017), H atoms were sprayed onto solid propynal at 10 K to examine reduction paths. To better quantify their experiments, the authors estimated three band strengths (*A*') by assuming that all the propynal vapor used in a deposition became part of the ice sampled by an IR beam. A comparison of the resulting three *A*' estimates with those we measured directly in our ices (Table 2) shows that those of Jonusas et al. (2017) are on average about 50% too small. This difference does not, however, change the main conclusions of those authors' paper.

Our work also applies to the results of Sivaraman et al. (2015), who irradiated solid propargyl alcohol at 85 K with 2 keV electrons. Peaks growing into their ice's IR spectrum near 2100 and 1666 cm^{-1} were not assigned, but using our Figs. 2, 3, and 5 we now attribute them to propynal's strong C≡C and C=O bands. The overall reaction is

$$HC{\equiv}C\text{-}CH_2OH \rightarrow HCC\text{-}C(O)H \quad (3)$$

analogous to the radiolytic decomposition of solid methanol

$$CH_3OH \rightarrow H_2CO \quad (4)$$

reported by many authors (e.g., Palumbo et al. 1999; Hudson & Moore 2000; Bennett et al. 2007; Chen et al. 2013; Sullivan et al. 2016).

It also is possible that the unusual intensity enhancement for propynal's C≡C band could be turned to astrochemical advantage and yield a solid-phase discovery by astronomical observers. For a previous paper we recorded IR spectra of a number of ices containing acetylene (HC≡CH, C_2H_2) in a search for this molecule's ν_3 (~3200 cm^{-1}, 3.125 μm) and ν_5 (~743 cm^{-1}, 13.46 μm) peaks in data from the Spitzer Space Telescope (Knez et al. 2012). However, our work was hindered by the quality of the Spitzer data available and the overlap of acetylene's bands with other IR features. To date, no molecule with a C≡C bond has been identified in an interstellar ice.

The IR spectra shown in the present paper suggest a different approach to alkyne detection in an interstellar ice, namely to consider propynal, a monosubstituted acetylene, instead of C_2H_2 itself. Propynal's strong C≡C band near 2100 cm^{-1} is near the ^{13}CO peak at ~2090 cm^{-1} in interstellar ices, but sufficiently separated for detection. The needed $\lambda / \Delta\lambda$ resolution is on the order of 200, much smaller than the 1000 or higher of the James Webb Space Telescope's NIRSpec instrument. Warmed ices depleted in CO could be inviting targets since propynal would remain after ^{13}CO was lost or diminished by sublimation. Even if a unique spectral assignment for propynal was impossible, this still suggests a chance for the first detection of an alkyne ice component in the interstellar medium and the possible observation of a carbonyl-containing ice component without having to rely on the crowded 1700 cm^{-1} IR region. Our demonstration of the relatively large strength of propynal's C≡C stretching feature suggests that it could, to some extent, offset a low abundance for this molecule.

We end with the three C_3H_2O isomers with which this paper began and which are shown in Fig. 1. An obvious question to ask is to what extent propynal in an ice can be induced to isomerize into either propadienone or cyclopropenone? Since propynal contains both a double and a triple bond, polymerization can be expected on exposing the solid compound to ionizing radiation or UV light, complicating efforts to identify C_3H_2O isomers. Difficulties could also arise on irradiating CO + C_2H_2 ice mixtures as each compound has been known for over a century to undergo reactions to make more-complex molecules, CO giving various suboxides and C_2H_2 making cuprene. – See the reviews of Reyerson & Kobe (1930) and Rasmussen (2017). – In analogy with photochemical studies (Stafast et al. 1985) radiolytic decomposition of propynal to CO and C_2H_2 also can be predicted. However, it still might be possible to demonstrate a radiolytic or photolytic isomerization such as

$$HCC\text{-}C(O)H \rightarrow H_2C{=}C{=}CO \quad (5)$$

if propynal were isolated in solid N_2, a rare-gas matrix, or even in H_2O-ice, experiments that remain to be done.

5 SUMMARY

Mid-IR spectra of solid propynal have been recorded under a variety of conditions for the first time, along with selected physical properties to help quantify the spectra. This new data can aid in the study of solid-phase isomerizations among the C_3H_2O isomers of Fig. 1, two of the isomers already having been identified in the interstellar medium. The strength and position of propynal's C≡C stretching band suggests that it could lead to the first identification of a molecule of its type in an interstellar ice.

ACKNOWLEDGMENTS

This work was supported by the NASA Astrobiology Institute through funding awarded to the Goddard Center for Astrobiology under proposal 13-13NAI7-0032. Marla Moore and Sarah Frail assisted with the propargyl alcohol irradiations. An anonymous reviewer is thanked for helpful comments.

REFERENCES

Allan J. L. H., Meakins G. D., Whiting M. C., 1955, JCS, 1874

Barros J., Appadoo D., McNaughton D., Robertson E. G., Medcraft C., Plathe R., Roy P., Manceron L., 2015, J. Molec. Spec., 307, 44

Bennett C. J., Chen S-H., Sun B-J., Chang A. H. H., Kaiser R. I., 2007, ApJ, 660, 1588

Benson R. C., Flygare W. H., Oda M., Breslow R., 1973, JACS, 95, 2772

Brand J. C. D., Watson J. K. G., 1960, JCS, 56, 1582

Brand J. C. D., Callomon J. H., Watson J. K. G., 1963, Disc. Farad. Soc., 35, 175

Brown R. D., Champion R., Elmes P. S, Godfrey P. D., 1985, JACS, 107, 4109

Chen Y-J., Ciaravella A., Muñoz Caro G. M., Cecchi-Pestellini C., Jiménez-Escobar A., Juang, K-J., Yih T.-S., 2013, ApJ, 778, 1

Claisen R. L., 1898, Ber. Deutsch. Chem. Gesell., 31, 1022

Costain C. C., Morton J. R., 1959, JCP, 31, 389

Denbigh K. G., 1940, Trans. Farad. Soc., 36, 936

Ekern, S., Szczepanski, J., Vala, M., 1996, JPC, 100, 16109

Gerakines P. A., Hudson R. L., 2015a, ApJ, 805, L20

Gerakines P. A., Hudson R. L., 2015b, ApJ, 808, L40

Giuliana B. M., Escribano R. M., Martín-Doménech R., Dartois E., Muñoz Caro G. M., 2014, A&A, 565, 108

Grindley T. B., Johnson K. F., Katritzky A. R., Keogh H. J., Thirkettle C., Brownlee R. T. C., Munday J. A., Topsom R. D., 1974, JCS Perkin 2, 276

Groner P., Stolkin I., Günthard H. H., 1973, J. Phys. E. - Sci. Instrum., 6, 122

Heavens O. S., 2011, Optical Properties of Thin Solid Films. 2nd edition, Dover, New York, p. 114. (Original printing: 1955, Butterworths Scientific Publ. London)

Hollenberg J., Dows D. A., 1961, JCP, 34, 1061

Hollis J. M., Remijan A. J., Jewell P. R., Lovas F. J., 2006, ApJ, 642, 933

Hudson R. L., Moore M. H., 2000, Icarus, 145, 661

Hudson R. L., Ferrante R. F., Moore M. H., 2014a, Icarus, 228, 276

Hudson R. L., Gerakines P. A., Moore M. H., 2014b, Icarus, 243, 148

Hudson R. L., Loeffler M. J., 2013, ApJ, 773, 773

Hudson R. L., 2016, PCCP, 18, 25756

Hudson R. L., Loeffler M. J., Gerakines P. A., 2017, JCP, 146, 0243304

Hudson R. L., Gerakines P. A., Ferrante R. F., 2018, Spectrochim. Acta, 193, 33

Irvine W. M., Brown R. D., Craig D. M., Fribery P., Godfrey P. D., Kaifu N., Matthews H. E., Ohishi M., Suzuki H., Takeo H., 1988, ApJ, 335, L89

Jonusas M., Guillemin J-C., Krim L., 2017, MNRAS, 468, 4592

Khanna R. K., Allen Jr. J. E., Masterson C. M., Zhao G., 1990, JPC, 94, 440

King G. W, Moule D., 1961, Spectrochim. Acta, 17, 286

Klaboe P., Kremer G., 1977, Spectrochim. Acta, 33A, 947

Knez C., Moore M. H., Ferrante R. F., Hudson R. L., 2012, ApJ, 748, 95

Lin C. T., Moule D. C., 1971, J. Molec. Spec., 37, 280

Loison J-C., Agúndez M., Marcelino N., Wakelam V., Hickson K. M., Cernicharo J., Gerin M., Roueff E., Guélin M., 2016, MNRAS, 456, 4101

Loomis R. A., McGuire B. A., Shingledecker C., Johnson C. H., Blair S., Robertson A., Remijan A. J., 2015, ApJ, 799, 34

Luna R., Millán C., Domingo M., Santonja C., Satorre, M., 2012, Vacuum, 86, 1969

McCarthy M. C., Zou L., Martin-Drumel M-A., 2017, JCP, 146, 154301

McKellar A. R. W., Watson J. K. G., Chu L-K., Lee Y-P., 2008, J. Molec. Spec., 252, 230

Molpeceres G., Satorre M. A., Ortigoso J., Zanchet A., Luna R., Millán C., Escribano R., Tanarro I., Herrero V. J., Maté B., 2017, MNRAS, 466, 1894

Moore M. H., Ferrante R. F., Moore W. J., Hudson R. L., 2010, ApJS, 191, 96

Nyquist R. A., 1971, Spectrochim. Acta, 27A, 2613

Pacansky J., England C. D., 1986, J. Phys. Chem., 90, 4499

Palumbo M. E., Castorina A. C., Strazzulla G., 1999, A&A, 342, 551

Pearson J. C., Drouin B. J., 2005, J. Molec. Spec., 234, 149

Petrie, S., 1995, ApJ, 454, L165

Pouchert, C., 1997, Aldrich Library of FT-IR Spectra, 2nd edition

Quan D., Herbst E., 2007, A&A, 474, 521

Rasmussen S., 2017, Bull. Hist. Chem., 42, 63

Reyerson L. H., Kobe K., 1930, Chem. Reviews, 7, 479

Richey C. R., Gerakines P. A., 2012, ApJ, 759, 74

Seburg R. A., Hodges J. A., and McMahon R. J., 2009, Helv. Chem. Acta, 92, 1626

Sivaraman B., Mukherjee R., Subramanian K. P., Banerjee S. B., 2015, ApJ, 798, 1

Stafast H., Pfister R., Huber J. R., 1985, J. Phys. Chem., 89, 5074

Sullivan K. K., Boamah M. D., Shulenberger K. E., Chapman S., Atkinson K. E., Boyer M. C., Arumainayagam C. R., 2016, MNRAS, 460, 664

Tempelmeyer K. E., Mills D. W., 1968, J. Appl. Phys., 39, 2968

Turner, B. E., 1991, ApJS, 76, 617

Veliev M. G., Guseinov M. M., 1980, Synthesis, 1980, 461

Wilks P. A., 1986 in Stock J. T., Orna M. V., eds, Chemists and Chemistry. Vol. 8, The History and Preservation of Chemical Instrumentation. Springer, Dordrecht, p. 27

Xie, H-B., Shao, C-B., Ding, Y-H., 2007, ApJ, 670, 449

Zhou L., Kaiser R. I., Gao L. G., Chang A. H. H., Liang M-C., Yung Y., 2008, ApJ, 686, 1493